Kuwait J.Sci., Vol.50, No.(1B),January.2023,pp(1-22)

Facies analysis and depositional framework of Late Permian-Jurassic sedimentary successions, Western Salt Range, Pakistan: implications for sequence stratigraphic trends and paleogeography of the Neo-Tethys Sea

Abdul Basit[1], Muhammad Umar[2, *], Muhammad Jamil[3,4], Muhammad Qasim[4]

[1]*Geological Survey of Pakistan, Quetta, Pakistan*
[2]*Dept. of Earth Sciences, The University of Haripur KPK, Pakistan*
[3]*Dept. of Geosciences, Universiti Teknologi PETRONAS (UTP), Seri Iskandar, 32610 Perak, Malaysia*
[4]*Dept. of Earth Sciences COMSATS University Islamabad, Abbottabad campus, Pakistan*

*****Corresponding Author: umarkhan09@yahoo.com*

Abstract

Facies analysis and T-R sequence stratigraphic approach of Late Permian to Jurassic sedimentary units in Western Salt Range, Pakistan were accomplished to construe the depositional environments and basin evolution. The analysis affirms the rendition of sequence stratigraphic trends and paleogeography of first megasequence phase of Neo-Tethys Sea. Sedimentological contingents, T-R sequence stratigraphic framework and sea level curve of the strata argue active tectonic's effects on sedimentation. During Late Permian, the rift related magmatic activities deceased, which imparted to the onset of transgression and deposition of shelf carbonates with retrogradational (transgressive) parasequence sets in Wargal Formation. Respective rifting and tectonic uplift events induced the sea level fall ascertaining the onset of terrigenous shelves and deltaic successions in terminal Permian and Early-Mid Triassic with an enlighten switch from agradational to progradational parasequence sets (regressive parasequences) in Chhidru, Mianwali and Tredian formations. The closure of Paleo-Tethys and emergence of semi-arid hot tropical climate throughout Late-Triassic, led the onset of tidal-lagoonal environments and deposition of retrogradational (transgressive) parasequence sets in Kingriali Formation. During Early Jurassic, a well-known northward drift of Pangaea ensued in global cooling and increased humidity, which consequently stimulated clastic-carbonate sedimentation of Datta and Samana Suk formations with progradational and retrogradational parasequence sets respectively.

Keywords: Basin evolution; depositional environments; neo-tethys sea; sequence stratigraphic trends; western salt range.

1. Introduction

The evolution of sedimentary basins is ascertained by variety of factors e.g., fluctuation in sea level (sequence stratigraphic trends), tectonics, paleogeographic position, and sediment influx (clastic or carbonate factories). Well exposed complete Late Permian-Jurassic successions in Western Salt Range (WSR) provide an opportunity to empathize the paleoenvironments, paleogeographic

evolution and sequence stratigraphic trends such as transgressive – regressive cycles, associated systems tracts and maximum flooding surfaces. These changes have induced the closure of Paleo-Tethys and opening of Neo-Tethys (Wignall & Hallam, 1993). Salt Range intends a well-distinguished fold-and-thrust belt, evolved at the South of the Himalayan foothills in response of an ongoing collision between Eurasian and Indian Plates (Baker *et al*., 1988; Farooqui *et al*., 2019; Qureshi *et al*., 2019; Umar *et al*., 2020). The Salt Range is regarded as the youngest compressional feature of Himalayan Foreland owing to its southward propagation. The generalized stratigraphy and tectonic settings are shown in the Figure 1.

A variety of sedimentary rocks e.g., sandstone, shale, limestone, and dolomite formed in different sedimentary environments through geologic time, ranged from Late Permian to Miocene in WSR. The Late Permian- Jurassic successions of WSR display clastic, siliciclastic and carbonate depositional systems. Various stratigraphic formations of the successions are delineated as source and producing reservoirs (e.g., Nazir *et al*., 2020) in various wells of Salt Range and Potwar Plateau. Facies/microfacies analysis, depositional architecture and sea level fluctuations play significant role in petroleum play analysis (Catuneanu & Zecchin, 2010; Umar *et al.*, 2016). Moreover, global, local tectonics and sea level fluctuations directly affected the sedimentation (Umar *et al*., 2011; Farooqui *et al*., 2022). The present study is planned to apply lithofacies/microfacies analysis to interpret depositional environments, tectonic influence on sedimentation and sequence stratigraphic framework of Late Permian-Jurassic strata.

2. Lithofacies-Microfacies Analysis

Five microfacies have been encountered in Wargal Formation (Figure 2a), denoted by WMF. These are Bioclastic wackestone-packstone, Bioclastic peloidal mudstone, Mudstone-wackestone, Calcic mudstone and Dolomitic mudstone microfacies (Table 1, Figure 2b-f). Bioclasts of bryozoans, bivalves, foraminifera, brachiopods, crinoids, gastropods, undifferentiated and micritized bivalves with allochems such as, ooids, peloids, interclasts and lumps are characteristic features of identified microfacies. These microfacies refers various shelf environments i.e., restricted middle-outer shelf, open marine, low energy inner shelf below fair-weather wave base, deep marine low energy and restricted lagoonal conditions (e.g., Scholle & Ulmer-Scholle, 2003; Flügel, 2004; Tucker, 2006). The distinguished five microfacies and lithofacies (Table-1) in mixed carbonate-clastic Chhidru Formation (Figure 3a) are Interbedded sandy mudstone and shale, Calcareous massive sandstone, Thick bedded massive sandstone lithofacies, Sandy Mudstone-Wackestone and Sandy Wackestone-Packestone Microfacies. Wackestone-Packstone, Mudstone fabrics, associated fauna (fusulinids, bryozoans brachiopod, gastropods), detrital grains and bioturbation (Figure 3b-i) in sandstone exhibit low energy calm proximal, open marine, tropical-subtropical, distal middle and inner shelf environments (Scholle & Ulmer-Scholle, 2003).

Six lithofacies and microfacies are discerned in Mianwali Formation (Figure 4a) included Dolostone, Ceratite Wacke-Packstone, Bivalve Wackestone Microfacies, Shale, Parallel and Cross laminated sandstone facies (Figure 4b-i). The existence of dolomite rhombs, conodonts, ceratite, gastropods, pelecypods, quartz grains, bioclasts of ammonoids, echinoderms, few glauconite,

peloids, grain supported fabric and mottling denote the open shallow marine, restricted to storm dominated inner shelf, low energy deeper part of inner and middle shelf (Scholle & Ulmer-Scholle, 2003; Milsom & Rigby, 2010; Iqbal *et al.,* 2014).

Table 1. Brief characteristics of identified lithofacies and microfacies with their corresponding depositional environments in Late Permian-Jurassic succession, WSR.

Formation Name	Facies/Microfacies	Description	Depositional Environments
Samana Suk Formation (Jurassic)	Mudstone Microfacies (SSM-1)	Medium bedded, light grey limestone, allochem deficient (<10%), mud-supported fabric with undifferentiated bioclasts	Middle shelf
	Peloidal/Pelletal Wackestone Microfacies (SSM-2)	Thin to medium bedded, yellowish grey limestone, mud-supported (>10% allochems) fabric, peloids and pellets	Peritidal-lagoonal
	Bioclastic Mud-Wackestone Microfacies (SSM-3)	Thin to medium bedded, grey limestone, mud-supported (<10% to <40% allochems) fabric with undifferentiated bioclasts	Lagoonal
	Packstone Grainstone Microfacies SSM-4	Medium bedded, dark grey sandy limestone, matrix deficient, grain-supported fabric with bioclasts and detrital grains (quartz)	Proximal inner shelf
Unconformity			
Datta Formation (Jurassic)	Massive sandstone facies (DF-1)	Medium-coarse grained sandstone, beds tabular with sharp bases and bed thickness increases upward	Lower shoreface
	Planar cross bedded Sandstone facies (DF-2)	Medium to thick bedded, coarse grained (coarsening up trend), planar cross bedding and pebbly bases	Deltaic distributary channels
	Rippled Sandstone interbedded with shale facies (DF-3)	Medium to thick bedded and coarse-grained sandstone interbedded with shale, bioturbation and asymmetrical ripples and shale beds up to 15 cm thick	Deltaic flood plain
	Trough cross bedded Sandstone (DF-4)	Thick bedded, medium-coarse grained sandstone with large scale trough cross bedding, channel fills and coarsening upward trend	Deltaic flood plain
	Carbonaceous Shale and coal facies (DF-5)	Dark brown shale, organic matter (plant remains)	Inter distributary bays and swamps of delta

	Bioturbated Sandstone facies (DF-6)	Fine to medium grained, medium bedded, intensely burrowed sandstone and thin organic rich shale interbeds	Distal mouth bar (delta front)
	Laterite facies (DF-7)	30-70 cm thick reddish laterite layers, indicate soil horizon	Sub-aerial exposure
Unconformity			
Kingriali Formation (Triassic)	Brecciated Dolostone (KMF-1)	Medium-thick bedded brecciated dolostone, fine-coarse grained with xenotopic (anhedral) crystals of dolomite, iron staining and evaporitic mold	Supratidal
	Peloidal Dolostone (KMF-2)	Thick beds of dolostone, olomicritic matrix with rounded-oval peloids and stromatoporoids with tabular to irregular fenestrae	Inter-subtidal
	Micritized Fenestral Dolostone (KMF-3)	Subhedral to anhedral crystals of dolomite with spherical to irregular fenestrae, stylolite and pyrite frambroids	Peritidal
	Dolomudstone (KMF-4)	Subhedral to anhedral crystals of fine-grained dolomite with spherical fenestrae and coralline stromatoporoids	Inter-subtidal
	Dolomitized Ooidal Grainstone (KMF-5)	Dolomitized tangential and micritic ooids, spar cement amongst the ooids is dolomitized	Subtidal
	Micritic Dolostone (KMF-6)	Subhedral-anhedral mosaic crystals of dolomite with irregular fenestrae, molds and partially dolomitized micrite with the presence of pellets, some stromatoporoids along with tabulate corals	Restricted lagoon
Unconformity			
Tredian Formation (Triassic)	Parallel laminated Sandstone interbedded Shale facies (TDF-1)	Medium to coarse grained sandstone interbedded with shale and carbonaceous material, parallel laminated, bioturbated, thickening & coarsening upward trend	Distributary channel
	Slumped Sandstone facies (TDF-2)	Medium grained sandstone, convoluted bedding and slumped structures	Delta front
	Cross laminated Sandstone facies (TDF-3)	Medium to coarse grained sandstone with low angle cross lamination, thickening and coarsening upward trend	Proximal delta front
	Large scale tabular cross bedded Sandstone facies (TDF-4)	Thick bedded, coarse-grained sandstone, lenticular channelized beds, large scale planar tubular cross bedding and coarsening upward trend	Delta plain
	Dolostone facies (TDF-5)	Medium-thick bedded and yellowish grey dolomite	Restricted shelf

	Laterite facies (TDF-6)	Lateritic soil horizon (40-60 cm thick), terrestrial fossils traces e.g., burrows of soil modifying organism and fossilized roots	Terrestrial Subaerial
Mianwali Formation (Triassic)	Dolostone Microfacies (MWF-1)	Medium bedded and fossiliferous dolostone, grain supported fabric and equigranular zoned rhombs of dolomite	Middle shelf
	Ceratite Wacke-Packstone Microfacies (MWF-2)	Thin bedded, highly fossiliferous limestone, mud to grain supported fabric, fragments of bivalves, ammonoids and gastropods	Inner shelf
	Shale facies (MWF-3)	Medium bedded shale with thin bedded limestone, siltstone, ammonoids, gastropods and bivalves	Shallow inner shelf
	Bivalve Wackestone Microfacies (MWF-4)	Medium bedded, fossiliferous limestone, mud supported fabric with bioclasts of bivalves, ammonoids (*ceratites*), echinoderms, gastropods, crinoids, glauconite and peloids	Deep inner shelf
	Parallel laminated Sandstone interbedded shale facies (MWF-5)	Medium bedded, fine to medium grained sandstone interbedded with shale, parallel lamination and bioturbation	Shallow inner shelf
	Cross laminated Sandstone facies (MWF-6)	Medium to thick bedded, fine to medium grained sandstone, cross lamination, erosive bases, channel fills, bioturbation and thickening upward trend	Deltaic Distributary channel
P-T boundary			
Chhidru Formation (Late Permian)	Interbedded sandy mudstone and shale facies (CHF-1)	Medium bedded sandy limestone with shale, mud supported fabric, allochmes of micritized bioclasts of fusulinids, bryozoans brachiopod and gastropods	Distal Middle shelf
	Calcareous massive Sandstone facies (CHF-2)	Medium-thick bedded, medium-coarse grained calcareous sandstone with bioclasts of brachiopods and bryozoans.	Proximal inner shelf
	Sandy Mudstone-Wackestone Microfacies (CHF-3)	Medium bedded sandy limestone, mud supported fabric with allochems of bryozoans, fusulinids and brachiopods	Proximal middle shelf
	Sandy Wackestone-Packestone Microfacies (CHF-4)	Medium bedded sandy limestone, grain supported fabric with allochems of detrital grains and bioclasts of fusulinids, bryozoans, brachiopods	Proximal middle shelf

	Thick bedded massive Sandstone facies (CHF-5)	Medium-coarse grained, massive sandstone, tabular bedding with sharp bases	Inner shelf
Wargal Formation (Late Permian)	Bioclastic Wackestone-Packstone Microfacies (WMF-1)	Grain supported, allochems (40-70%) include bioclasts of bryozoans, brachiopods, crinoids and gastropods	Middle shelf
	Bioclastic Peloidal Mudstone Microfacies (WMF-2	Allochem deficient (<10%), mud supported, allochems includes ooids, peliods, fragments of bryozoans, crinoids, brachiopods and foraminifers	Restricted Inner shelf
	Mudstone-Wackestone Microfacies (WMF-3)	Allochem deficient, mud supported, allochems are bioclasts of brachiopods, bryozoans, bivalves, crinoids and gastropods	Inner shelf
	Calcic Mudstone Microfacies (WMF-4)	Allochem deficient (<10%), mud supported, undifferentiated micritized and reworked or fragmented bioclasts	Outer shelf
	Dolomitic Mudstone Microfacies (WMF-5)	Mud supported, pre mature dolomitization of mud, fauna absent, micritization and recrystallization	Middle lagoonal shelf

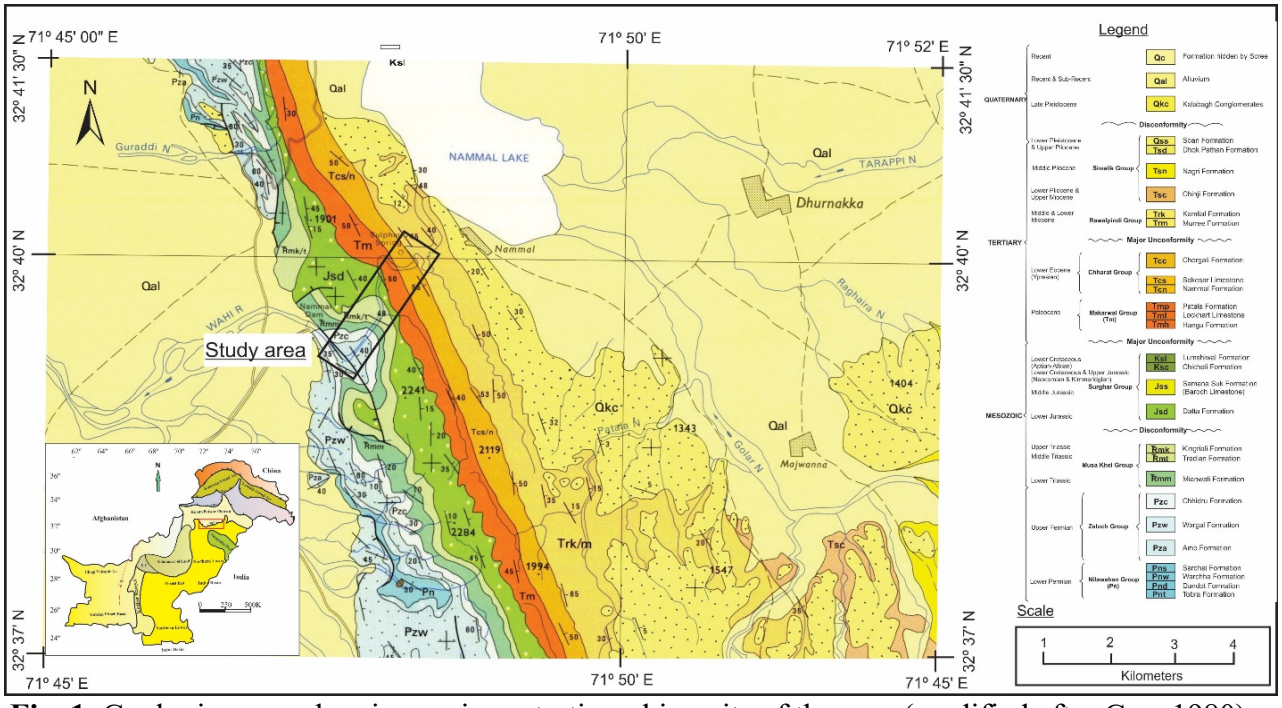

Fig. 1. Geologic maps showing various stratigraphic units of the area (modified after Gee, 1980).

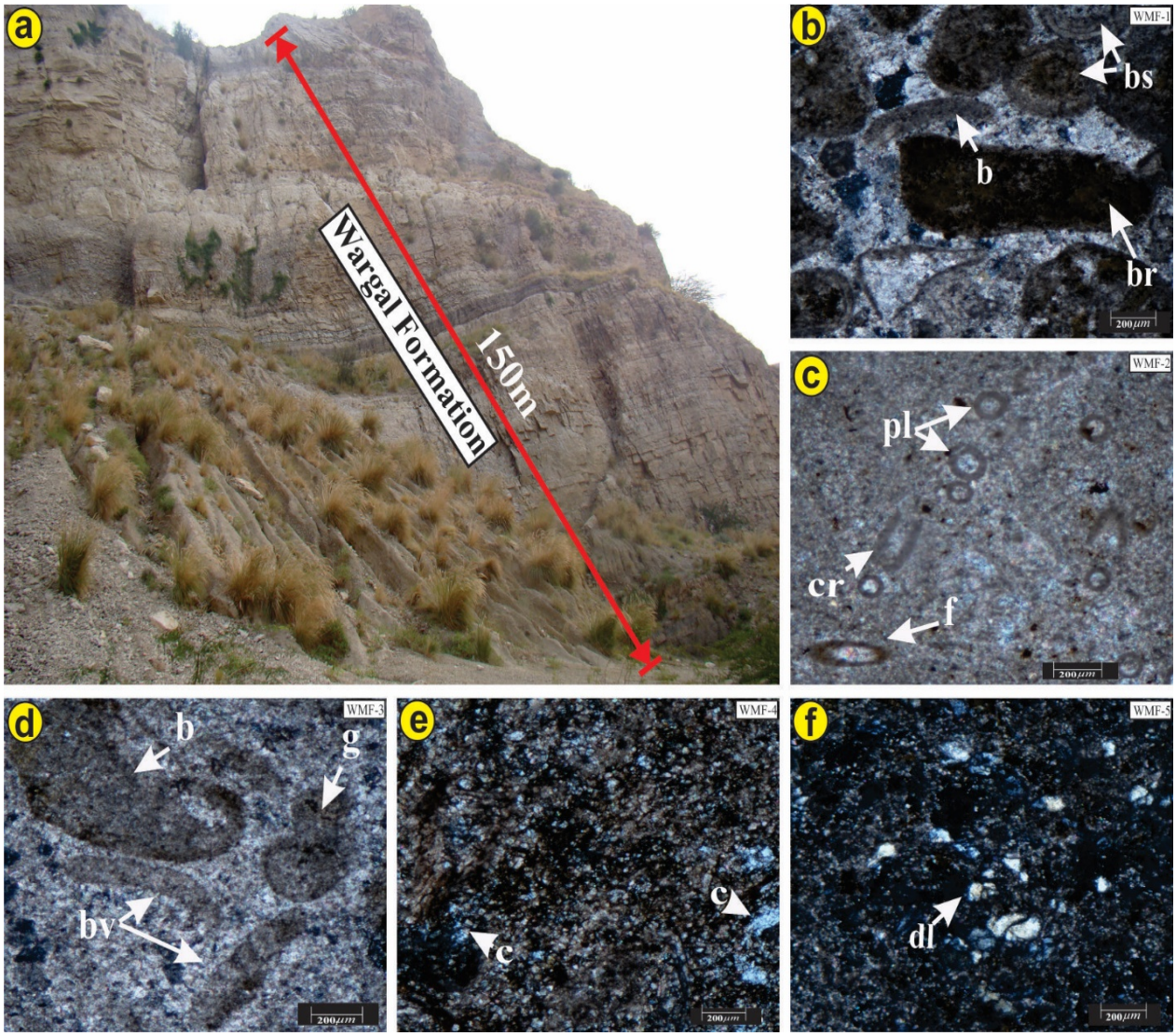

Fig. 2. (a) Field photograph showing general view of the Wargal Formation; (b) Photomicrograph of bioclastic wacke-packstone fabric of WMF-1, brachiopod spines (bs), brachiopod (b), bryozoans(br); (c) Photomicrograph indicates bioclastic peloidal mudstone microfacies (WMF-2), peloids (pl), crinoid (cr), foraminifera (f); (d) Photomicrograph of mudstone-wackestone microfacies (WMF-3) with bioclasts of bivalve (bv), gastropod (g), brachiopod (b); (e) Photomicrograph of calci mudstone fabric of WMF-4 and (f) Photomicrograph of dolomitic mudstone microfacies (WMF-5) dolomite crystals (dl).

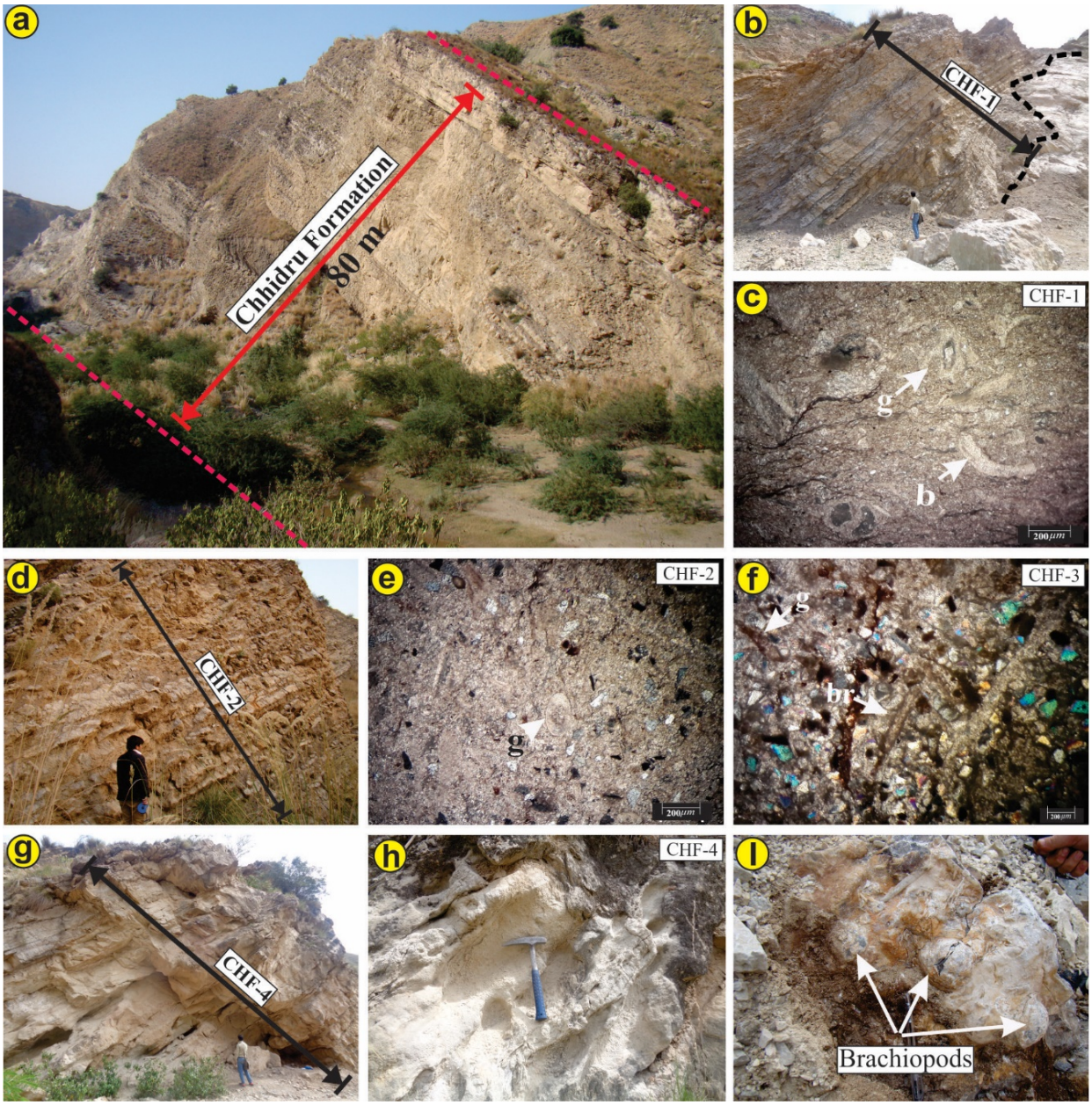

Fig. 3. (a) Field photograph showing exposure of Chhidru Formation; (b) Field photograph of interbedded fossiliferous mudstone facies (CHF-1) of Chhidru Formation; (c) Photomicrograph shows mud supported rock fabric with bioclasts of brachiopods (b), bryozoans (br), fusulinids (f) in CHF-1; (d) Field view of sandy mudstone-wackestone microfacies (CHF-2); (e) Photomicrograph exhibits sandy mudstone-wackestone fabric with gastropods fragments and undifferentiated bioclasts of CHF-2; (f) Photomicrograph of sandy wackestone-packstone fabric of CHF-3 with bioclasts of gastropods (g), bryozoans (br) and other undifferentiated bioclasts; (g) Field photograph of calcareous massive sandstone facies (CHF-4); (h) Field view of massive white colored sandstone of calcareous massive sandstone facies (CHF-4) and (i) Field view of shells of brachiopods in interbedded fossiliferous mudstone facies (CHF-1).

Laminated shale with thin limestone interbeds, parallel and cross laminated sandstones were formed in open marine, inner shelf and distributary channels of delta. Lithofacies recognized in Tredian Formation (Figure 5a), are parallel laminated sandstone interbedded with shale, slumped sandstone, cross laminated sandstone, large scale tabular cross bedded sandstone, dolomite and laterite facies (Oxisols) (Figure 5b-i). Sandstone of the formation is medium to thick bedded, parallel & cross laminated, cross stratified, lenticular, channelized, bioturbated exhibiting a coarsening/thickening upward trend. The sandstones were formed by wave & current actions, variation in flow velocities, suspension and traction processes in proximal delta front to continental delta plain. Slumped sandstone was reckoned owing to slope failure along steep channels and banks causing soft sediments deformation. Dolomite and laterite facies represent the restricted shelf and soil horizon respectively. Kingriali Formation (Figure 6a) is categorized into Brecciated dolostone**,** Peloidal dolostone, Micritized fenestral dolostone, Dolomudstone, Dolomitized ooidal grainstone and Micritic dolostone microfacies (Figure 6b-f). The significant features of recognized microfacies are brecciated dolomite, dolomitic limestone, two-phased dolomites, evaporitic molds, stromatoporoids, xenotopic, hypidiotopic, idiotopic crystals, jigsaw puzzle structures, rounded to oval peloids, spherical to irregular fenestrae fabric, pyrite frambroids, tangential & radial ooids, gastropods, pelecypods, tabulate corals and some intraclasts. Dolomites were primary and diagenetic in origin. The formation was deposited in supratidal, intertidal – subtidal, peridal, high energy inner shelf/ramp environments.

Terrigenous Datta Formation (Figure 7a) is characterized by Massive sandstone, Bioturbated sandstone, Planar cross bedded, Trough cross bedded sandstones, Rippled sandstone interbedded with shale, Carbonaceous shale and Laterite facies (Table 1; Figure 7b-i). The Formation depicts fine to medium grained, medium bedded, massive, intensely burrowed sandstone with few centimeters thick organic rich beds and were likely consociated with flood plain and proximal part of deltaic front settings. Coarse grained large scale planar cross bedded sandstone was produced by downstream movement of dune associated with unidirectional high velocity flow (Umar *et al*., 2011; 2016) in point bars and channel bars, topsets areas of deltaic system. Rippled sandstone interbedded with shale facies was formed by unidirectional flows associated with rivers and streams, longshore currents and backwash on beaches (Boggs, 2014). Trough cross bedded sandstone, channel fills and conglomeratic bases indicate migration of large dunes commonly associated with channel belt facies of deltaic plan environment (Boggs, 2014). Carbonaceous shale facies, interbeds of siltstone and organic matter in the form of plant remains and imprints of leaves were generally associated with low energy conditions of flood plains, swamps and inter-distributary bays of deltaic environments (e.g., Abbasi *et al*., 2012). Red color laterite, sandy and clayey soil were produced due to extensive weathering of bed-rock. The repeating trend of laterite beds attest various episodes of subaerial exposures (Kasi *et al*., 2018) and most probably associated with deltaic depositional settings. Carbonate rich Samana Suk Formation (Figure 8a) is dissevered into Mudstone, Peloidal/Pelletal wackestone, Bioclastic mud-wackestone and Wackestone-packstone microfacies (Figure 8b-f). Peliods and wackestone fabric refer low energy restricted peritidal-lagoonal environment (Scholle & Ulmer-Scholle, 2003; Khan *et al.*, 2021). Bioclastic Mud-Wackestone depositional fabric and fauna reveal low energy shallow

water lagoonal environments. Wackestone-Packstone Microfacies include recrystallized bioclasts and detrital quartz grains which display the proximal inner ramp settings with high energy fluvial influence.

3. Discussion

3.1 Sequence stratigraphic analysis

The studied succession furnishes an examples of stacking pattern of parasequence sets (Embry & Johannessen, 1992) to reveal Regressive System Tract (RST) and Transgressive System Tract (TST). Nineteen (PS-1 to PS-19) parasequences were distinguished in Late Permian to Jurassic succession in WSR (Figure 9). Haq *et al*. (1988) have intended the chronostratigraphy and global cycles of sea level changes during Mesozoic and Cenozoic eras. Few meters rise in base level at terminal Permian time caused the deposition of TST in Wargal Formation with retrogradational (transgressive) parasequrnce sets (Figure 9). Three TST and two RST were distinguished on the basis of parasequence stacking pattern and facies architecture. First TST with retrogradational parasequence stacking pattern of the cycle is marked along complete strata of the wargal formation. Basal shallow water parasequences (PS-1 to PS-3) are overlain by upper deep water parasequences (PS-4, PS-5; Figure 9). Chhidru Formation was deposited at the regressive phase when base level was at lowest stage during terminal Permian. The regressive event was detected by increased terrigenous influx to the shelf throughout the deposition of Chhidru and Mianwali formations. Complete shift had occurred during deposition from shelf (Mianwali Formation) to fluvio-deltaic (Tredian Formation). Global rise as well as small scale and short-term falls in sea level during Early to Middle Triassic were attested by Haq *et al*. (1988, 2017). Soil horizon at top of Tredian Formation destines subaerial exposure and argues the sequence boundary (an unconformity). The succeeding transgressive cycle was corresponded to deposition of the Kingriali Formation in shallow water supratidal-intertidal facies overlain by subtidal-lagoonal facies. This parasequence sets was deposited throughout transgressive episode and make TST for succeeding cycle. The depositional setting was wobbled from tidal/ lagoonal to fluvio-deltaic during Early Jurassic (Datta Formation) in regression phase (RST). The topmost soil horizon of the formation exhibits an unconformity interpreted as sequence boundary (SB). Transgressive cycle was commenced merely over (DF-7) when carbonate-rich Samana Suk Formation was deposited in shelf/lagoon environments.

Two T-R Sequences were discerned in studied successions (Figure 10). T-R Sequence-I includes Wargal (TST), Chhidru, Mianwali and Tredian formations (RST). Maximum flooding surface (MFS) is interpreted at the contact between WMF-4 and WMF-5 (Table-1) in the upper part of the Wargal Formation (Figure 9). Soil horizon at the top of Tredian Formation deputes the termination of RST, sequence boundary (SB) of TR sequence (Embry & Johannessen, 1992) and sub-aerial unconformity in terminus Middle Triassic owing to short term and local regression phases. The succeeding T-R Sequence-II incorporated to Kingriali (TST) and Datta formations (RST). Maximum Flooding Surface (MFS) at the top of Kingriali Formation (between KMF-6 and DF-1; Table-1) separates the TST from overlying RST (Embry & Johannessen, 1992). The

deposition of Kingriali Formation illustrated the Late Triassic transgressive phase of Haq *et al*. (1988).

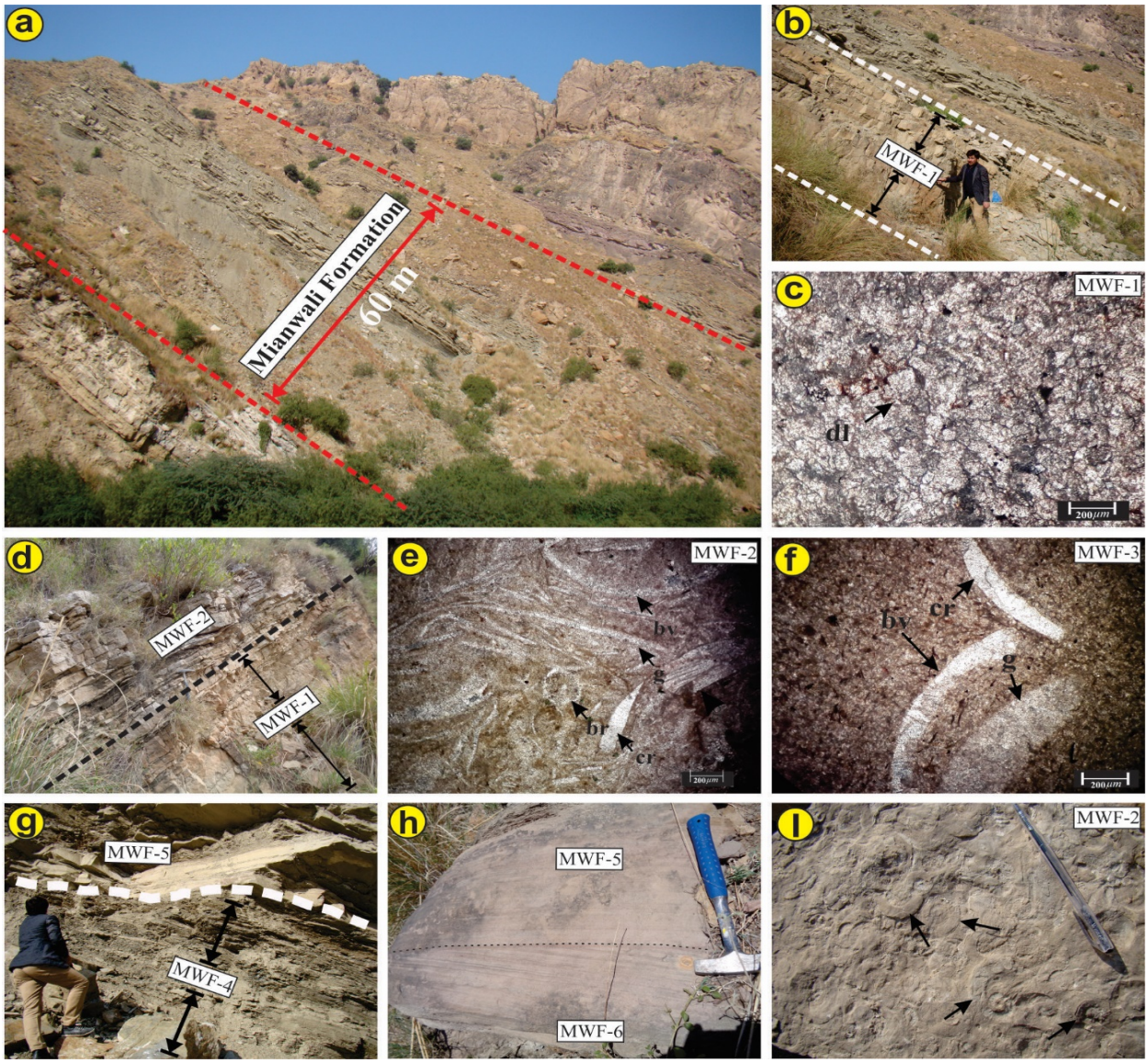

Fig. 4. (a) General view of Mianwali Formation; (b) Medium bedded dolomite of MWF-1; (c) Photomicrograph showing dolomite grains of MWF-1; (d) Field view thin bedded fossiliferous limestone of MWF-2; (e) Photomicrograph of bioclastic wackestone-packstone fabric of MWF-2, bioclasts of gastropods (g), bivalves (bv), brachiopods (br), crinoids (cr); (f) Photomicrograph of mud supported bioclastic wackestone fabric of MWF-3, bioclasts of bivalves (bv); (g) Field Photograph of shale (MWF-4) and overlying parallel laminated sandstone interbedded shale facies (MWF-5) (h) Field photograph showing cross laminated sandstone facies (MWF-6) overlain by (MWF-5); (i) Field view of fossiliferous bed of ceratite wacke-packstone microfacies (MWF-2).

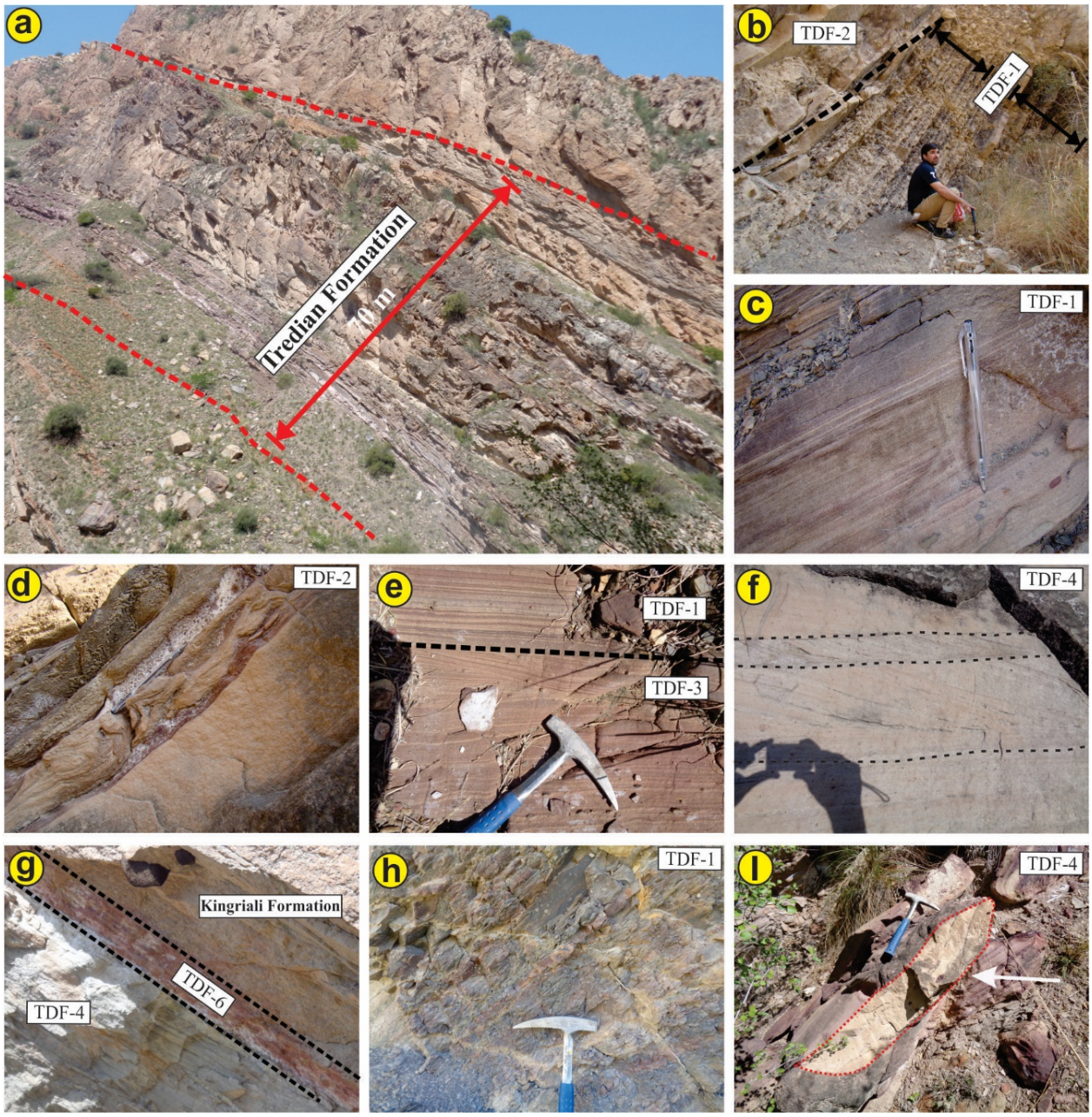

Fig. 5. (a) Field photographs of Tredian Formation; (b) Parallel laminated sandstone interbedded shale facies; (c) Parallel laminated sandstone of TDF-1; (d) Slumped sandstone facies (TDF-2); (e) Cross laminated sandstone of TDF-3; (f) Large scale tabular cross bedded sandstone facies (TDF-4); (g) soil horizon/laterite bed of TDF-6 at the top of Tredian Formation; (h) Carbonaceous material in shale of (TDF-1); (i) Channel structures in (TDF-4).

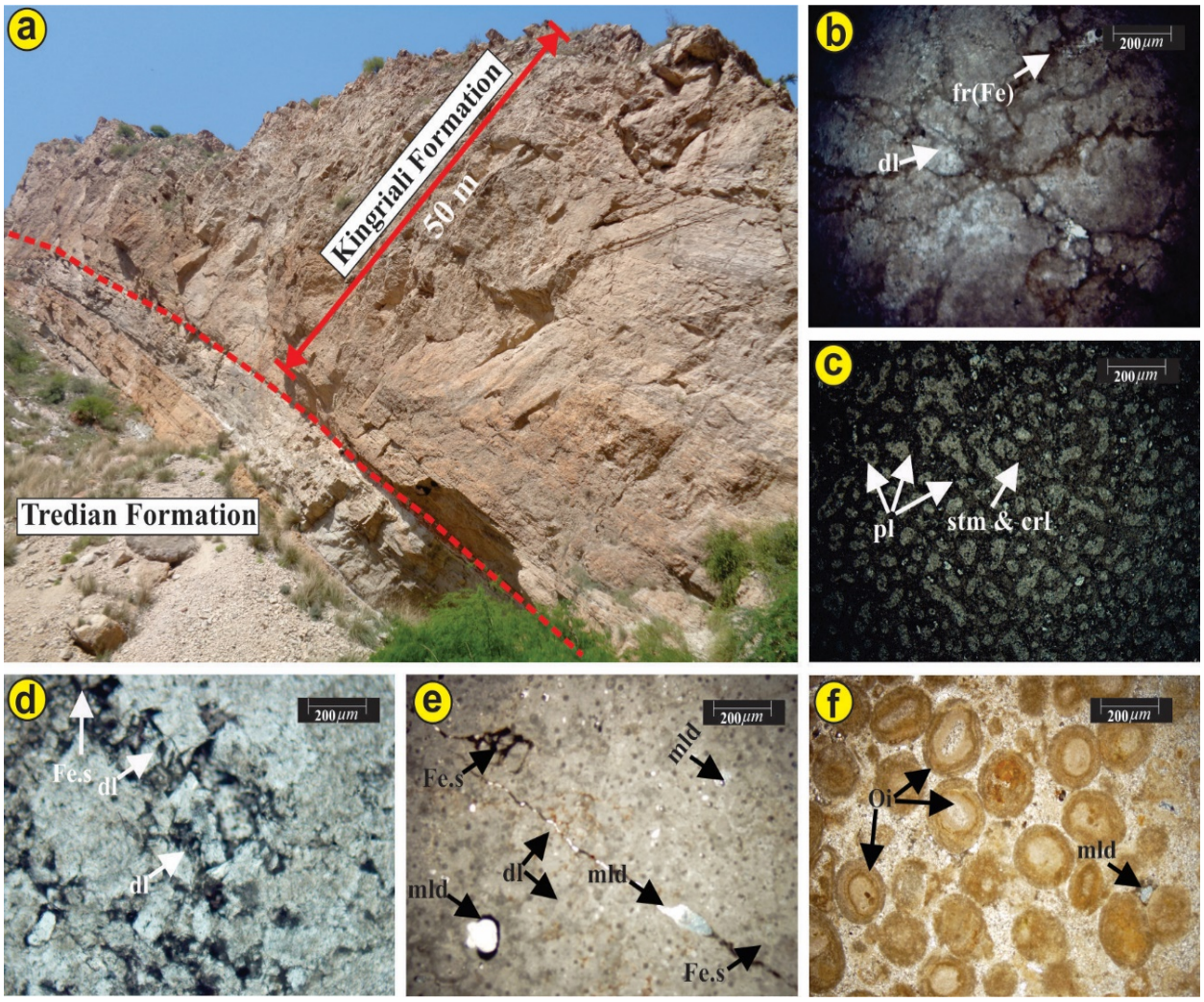

Fig. 6. (a) General view of the Kingriali Formation; (b) Photomicrographs of brecciated dolostone microfacies (KMF-1) with fine to coarse grained anhedral dolomite (dl) crystals with fractures (fr) and fractures filled with iron (Fe); (c) Peloidal dolostone microfacies (KMF-2) with pl; peloids with co-existence of stromatoporoids (stm) and corals (crl); (d) Micritized fenestral dolostone microfacies (KMF-3) with fine to coarse grained, subhedral to anhedral dolomite (dl) crystals with Iron staining (Fe.s); (e) Dolomudstone (KMF-4) with molds (mld) and iron staining (Fe.s); (f) Dolomitized ooidal grainstone microfacies (KMF-5) with tangential, radial and micritic ooids with bioclasts.

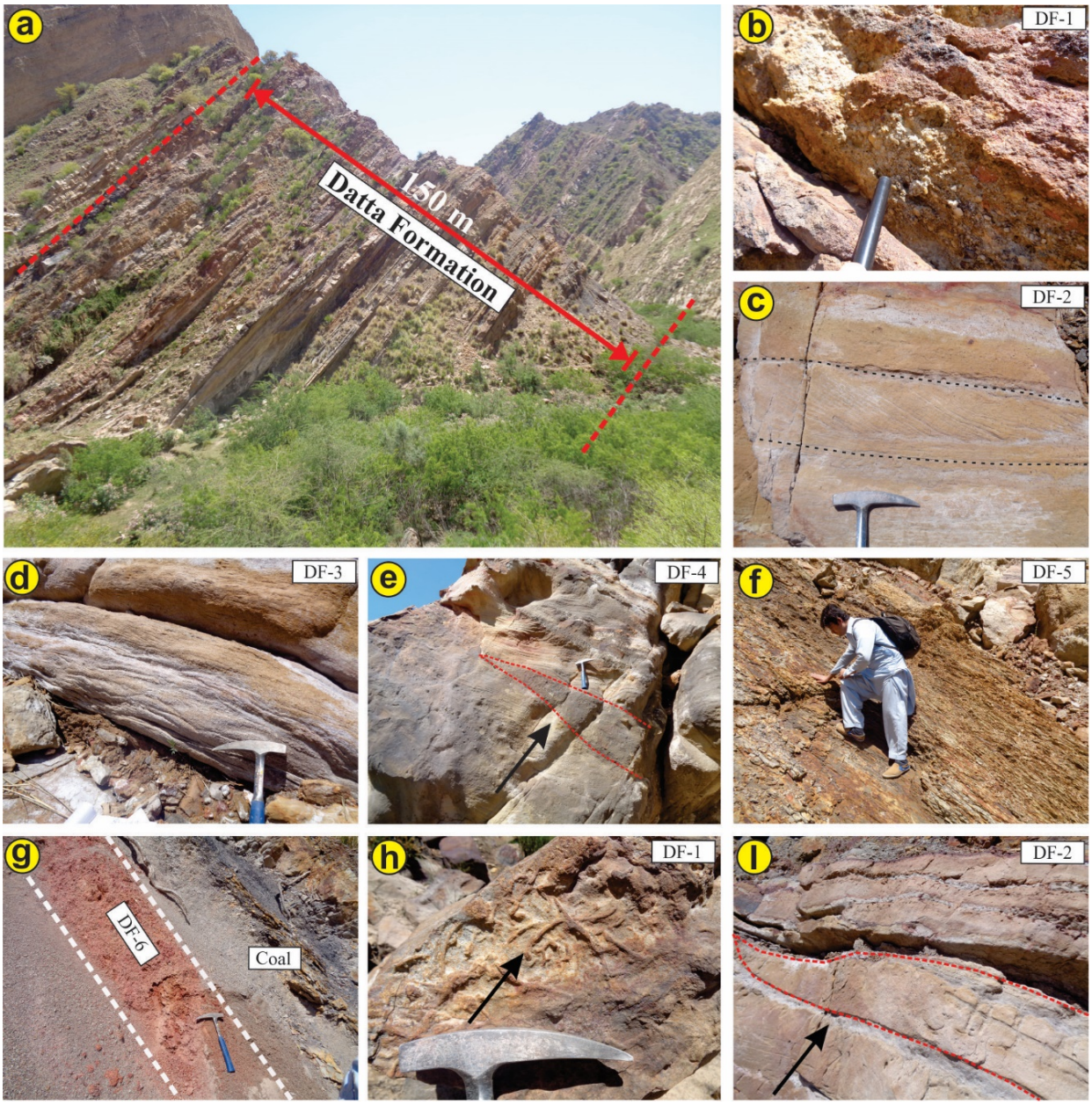

Fig. 7. (a) Field photograph showing outcrop exposure of Datta Formation; (b) View of massive sandstone facies (DF-1) with pebbly base; (c) Field photograph of planar cross bedded sandstone facies (DF-2); (d) Field photographs of rippled sandstone interbedded with shale facies (DF-3); (e) Trough cross bedded sandstone with channel structure (DF-4); (f) Shale of carbonaceous shale and coal facies (DF-5); (g) Laterite bed of laterite facies (DF-7); (h) Burrows in (TDF-1); (i) Channelized beds in (TDF-2).

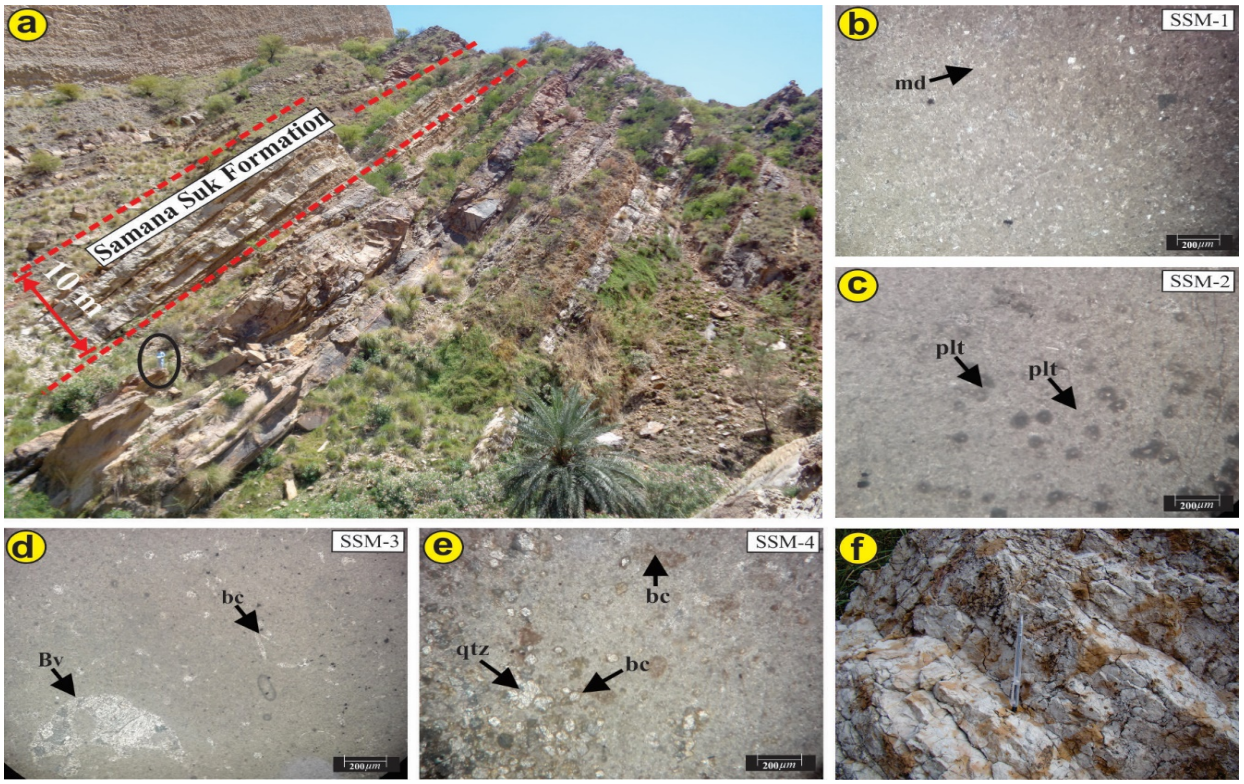

Fig. 8. (a) Field photograph shows exposure of Samana Suk Formation; (b) Photomicrograph of mud supported fabric of mudstone microfacies (SSM-1); (c) Mud supported and peloid and pellet containing fabric of peloidal/pelletal wackestone microfacies (SSM-2); (d) Bioclastic containing mud supported fabric of bioclastic mud-wackestone microfacies (SSM-3); (e) Wackestone-packstone microfacies (SSM-4); (f) Filed view of limestone of Samana Suk Formation

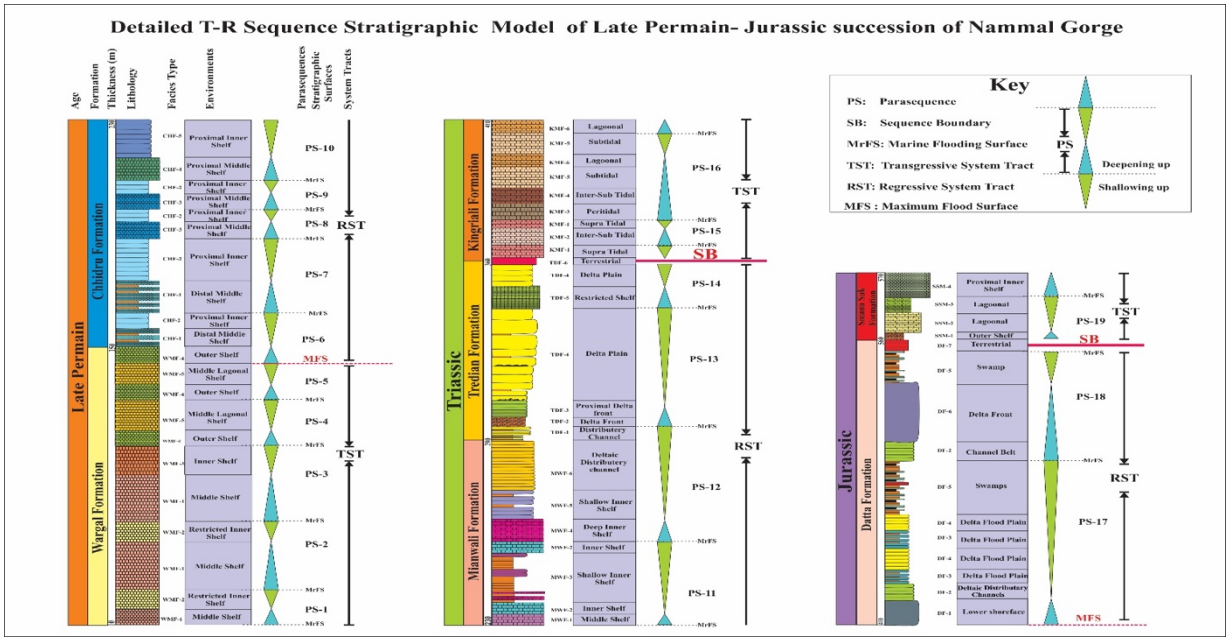

Fig. 9. Detailed Facies Architecture and T-R Sequence Stratigraphic Analysis.

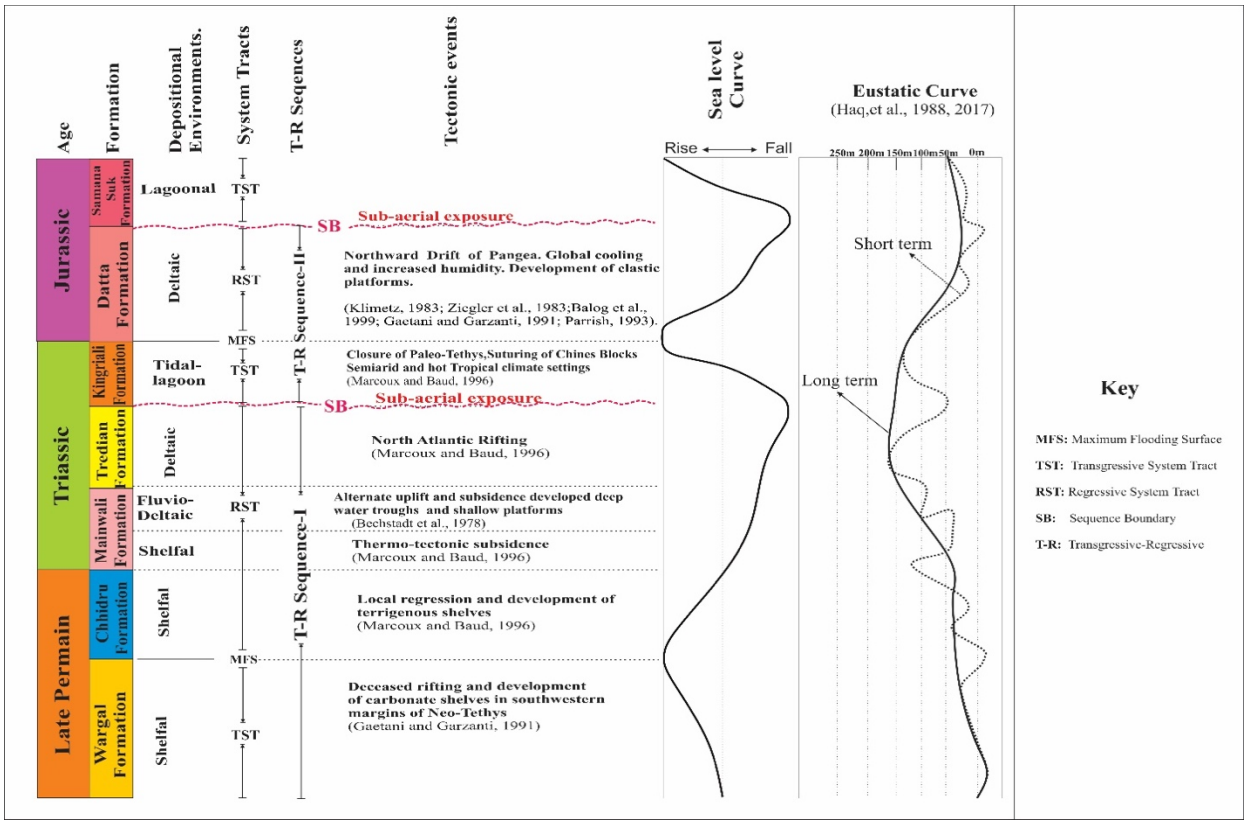

Fig. 10. T-R Sequence Stratigraphic Analysis and its relation to Tectonics and Sea Level Fluctuations of Late Permian-Jurassic rocks of studied area (modified after Haq *et al*., 1988, 2017).

The soil horizons in Datta Formation stigmatize cessation of Regression and Sequence Boundary of T-R Sequence-II. Global regression flux in Early Jurassic was manifested by regressive phase deposition of Datta Formation. Samana Suk Formation corresponded to transgressive phase of next T-R cycle.

3.2 Tectonic control on sedimentation

Stratigraphic succession exposed in various sedimentary basins, revealed the tectonic and depositional evolution of Indian Plate particularly during Permian-Jurassic time span in response to rifting of Gondwana, separation of Cimmerian Block and opening of Neo-Tethys Ocean. Terrigenous and carbonate sedimentation within sedimentary basins developed in response to episodic rifting of Gondwana super-continent through Carboniferous-Jurassic (Zeigler, 2015). The Gondwanian sedimentary rocks of Indian Plate were substantially correlated with terrains exposed in Madagascar, Eastern Africa, Seychelles, Arabian Peninsula and Indus Basin (including studied area) (Bhattacharya & Bhattacharya, 2015). Tectono-sedimentation in Carboniferous-Jurassic can be reconstructed e.g., western India was colligated with Madagascar, Africa, Arabia, and Seychelles Plates (Mukherjee, 2017), was moved towards North (near equator) in terminal Triassic (Torsvik & Cocks, 2013). North-South rifting induced crustal extension throughout Carboniferous – Permian and premised the breakup of Gondwana super-continent (Delvaux, 1991). Based on GIS

study, the linear disposition of Dwyka (South Africa), Al-Khalata, Gharif (Oman), Sakoa (Madagascar) and Nilawahan (Western Salt Range) formations, parallel faults trend to such lithostratigraphic units, persistence, resemblance of lithologies and structures exhibit the probable existence of Gondwana rift. The notion intends comparable tectono-sedimentary environments in South Africa, Oman, Madagascar, and Western Salt Range. Extension of such rift and separation of Cimmerian block were developed Neo-Tethys Ocean, North of India in Mid Permian–Early Triassic (Torsvik & Cocks, 2013). Basement ridges in Indus basin (Delhi-Lahore-Sargodha) were uplifted in Mid Permian (Asim *et al*., 2014).

Precambrian - Early Permian sedimentation on the Indian Plate, within Paleo-Tethys was shifted to Neo-Tethys in Late Permian due to final detachment of India from Gondwana and opening of Indian Ocean (Gaetani & Garzanti, 1991). The opening of Neo-Tethys was consorted with Early Permian extensional magmatic activity. The termination of magmatic activity succeeded to the deposition of transgressive parasequence sets of Wargal Formation in newly evolved Neo-Tethys shelf. In addition, shallow water carbonate platform was well established in Salt Range within Neo-Tethys between 30°N and 30°S. Terrigenous deposits of Chhidru Formation are comparable with clastic shelves of India and northwest Australia during Late-Permian due to local regressive cycle of T-R sequence (Marcoux & Baud, 1996). Thermo-tectonic subsidence and rift related submergence in Early Triassic (Gaetani & Garzanti, 1991; Marcoux & Baud, 1996) led to the deposition of MWF-1 and MWF-2 of Mianwali Formation in inner continental margin. Rapid shallowing upward conditions were acquired in Anisian and Ladinian (Mid-Triassic) owing to uplift, which ensued a complex pattern of deeper troughs and shallow water platforms (Bechstadt *et al*., 1978). On account of this composite pattern of deposition, a rigorous shift from under-fill to overfill basin (Lawa *et al*., 2013) is depicted in the form of shelf facies overlain by deltaic facies in Mianwali Formation with its regressive parasequence sets. North Atlantic rifting through Norian was inducted the clastic sedimentation in the Neo-Tethys (Marcoux & Baud, 1996) as marked in Tredian Formation and alike clastics in the other sedimentary basins of India (Gaetani & Garzanti, 1991). High sediments load and low accommodation space triggered the overfilling of basin up to subaerial exposure as exemplified by soil horizons (TDF-6) at the top of Tredian Formation and marks the end of regression. Furthermore, sub-aerial exposure (soil horizon) in WSR and Indian basin was recorded at Norian-Rhaetian Boundary. Late Triassic global tectonics demonstrate the commencing of Pangaea's breakup and occlusion of Paleo-Tethys (Fan *et al*., 2017) on account of northward drift of Cimmerian Plate, its convergence and suturing with Chinese Blocks led to the growth of large carbonate platform in Neo-Tethys margins (Ghosh *et al*., 2016; Sardar Abadi *et al*., 2019; Enayati-Bidgoli & Navidtalab, 2020). The subtidal/lagoonal dolomitization (Kingriali Formation), owing to semiarid and hot tropical climate conditions in transgressive parasequence sets was resulted by such tectonostratigraphic event. Late Triassic Dolostone units were deposited in Central Asia (Fan *et al*., 2017; Borrelli *et al*., 2019; Enayati-Bidgoli & Navidtalab, 2020) is comparable with Kingriali Formation. Global cooling and humidity increase owing to well-documented northward movement of Pangea, the dolomitization abruptly quitted at the end of Triassic (Gaetani & Garzanti, 1991). The similar cessation of dolomite was observed at the top of Triassic Kingriali Formation in WSR. Sedimentation in Early Jurassic depicts shift from tidal-

lagoonal to deltaic facies of Datta Formation. The condensed black shale at the base of Datta formations signs the maximum flooding surface across which the change from transgressive to regressive parasequence sets is obviously manifest (Omar *et al*., 2015). In Early Jurassic till Late Callovian, high sediments supply but low accommodation space stimulated sub-aerial exposure and development of laterite beds. Such subaerial exposure is distinguished by existence laterite beds (DF-7) at the top of Datta Formation correspond to referred episode of sedimentation in Neo-Tethys. A Transgressive episode was commenced in terminal Callovian and shelf carbonate platforms ensued to form in Late Jurassic. Samana Suk Formation was accumulated during such episode of sedimentation (Khan *et al*., 2021) in Neo-Tethys Ocean.

4. Conclusions

1. Lithofacies, microfacies, sequence stratigraphic framework and sea level curve of Late Permian to Jurassic strata Western Salt Range, contend the tectonic consequence on sedimentation.

2. The Wargal Formation dominantly compiled the mudstone, mud-wackestone, wackestone-packstone and dolomitic mudstone depositional fabrics corresponding to lagoonal and restricted inner to outer shelf environments. The microfacies of the formation exhibit retrogradational depositional architecture inducing TST of T-R Sequence-I. Mixed clastic – carbonate sedimentation in the Chiddru Formation constitutes regressive phase sequence throughout Late Permian period.

3. Early Triassic Mianwali Formation typifies RST with progradational depositional architecture in clastic-carbonate mixed succession. Terrigenous-rich Tredian Formation was accumulated in fluvio-deltaic environments as attested by defined lithofacies e.g., large-scale cross bedded, cross laminated, parallel laminated sandstones interbedded with shale and slumped sandstone facies. The soil horizons signal sub-aerial exposure and set the sequence boundary. Tidal – lagoon settings were acquired due to closure of Paleo-Tethys, suturing of Chines Blocks and development of semi-arid hot tropical climate in Late Triassic time. Dolomite-rich Kingriali Formation was deposited in the same environments. The boundary between Tredian and Kingriali formations signs the sequence boundary and initiate transgressive episode of next T-R Sequence-II.

4. Global cooling and humidity enhancement owing to northward drift of Pangea and led to development of clastic-carbonate successions in Early Jurassic. The distinguished lithofacies of Datta Formation display fluvio-deltaic environments. The formation corresponds to RST of T-R Sequence-II, whereas the laterite beds represent sub-aerial exposure and marked the sequence boundary. Samana Suk Formation represents the transgressive phase of succeeding cycle.

5. Sedimentation of Late Permian - Jurassic strata, WSR was tempted by active tectonic and most probably correspond to rifting of Gondwana, separation of Cimmerian block, opening of Neo-Tethys Ocean, northward drift of Pangea and suturing of Chinese Blocks.

References

Abbasi, I.A., Haneef, M., Obaid, S., Daud, F., & **Qureshi, A.W. (2012)** Mesozoic deltaic system along the western margin of the Indian Plate: lithofacies and depositional setting of Datta Formation, North Pakistan. Arabian Journal of Geosciences, 5(**3**), 471-480.

Asim, S., Qureshi, S.N., & **Khan, N. (2014)** Study of an uplift of Sargodha High by stratigraphical and structural interpretation of an east-west seismic profile in Central Indus Basin, Pakistan. International Journal of Geoscience, 5(**9**), 1027.

Baker, D.M., Lillie, R.J., Yeats, R.S., Johnson, G.D., Yousuf, M., & **Zamin, A.S.H. (1988)** Development of the Himalayan frontal thrust zone: Salt Range, Pakistan. Geology, 16(**1**), 3-7.

Bechstadt, T., Brandner, R., Mostler, H. & **Schmidt, K. (1978)** Aborted rifting in the Triassic of the Eastern and Southern Alps, Neues Jabrbuch fur Geologie und Palaontologie Abhandlungen, 156, 157-178.

Bhattacharya, H.N., & **Bhattacharya, B. (2015**) Lithofacies architecture and paleogeography of the Late Paleozoic glaciomarine Talchir Formation, Raniganj Basin, India. Journal of Paleogeography, 4(**3**), 269-283.

Boggs, S. (2014) Principles of Sedimentology and Stratigraphy, 5th Edition. Pearson Publisher, 598.

Borrelli, M., Campilongo, G., Critelli, S., Perrotta, I.D., & **Perri, E. (2019)** 3D nanopores modeling using TEM-tomography (dolostones-Upper Triassic). Marine and Petroleum Geology, 99, 443-452.

Catuneanu, O., & **Zecchin, M. (2010)** High resolution sequence stratigraphy of clastic shelves III: Application to reservoir geology. Marine and Petroleum Geology, 62, 161-175.

Delvaux, D. (1991) The Karoo to Recent rifting in the western branch of the East-African Rift System: A bibliographical synthesis. Rapport Annuel 1989-1990, de Geologie et Mineraloqie, Musee Royale de I'Afrique Centrale, Tervuren, Belgium, B-3080, 63-83.

Embry, A.F., & **Johannessen, E.P. (1992)** T-R sequence stratigraphy, facies analysis and reservoir distribution in the uppermost Triassic-Lower Jurassic succession, western Sverdrup Basin, Arctic Canada. In: Vorren, T. O., Berg - Sager, E., Dahl-Stamnes, O. A., Holter, E., Johansen, B., Lie, E., Lund, T. B. (Eds.), Arctic Geology and Petroleum Potential. Norwegian Petroleum Society (NPF) Special Publication, 2: 121–146.

Enayati-Bidgoli, A., & **Navidtalab, A. (2020)** Effects of progressive dolomitization on reservoir evolution: A case from the Permian–Triassic gas reservoirs of the Persian Gulf, offshore Iran. Marine and Petroleum Geology, 119, 104480.

Fan, J.J., Li, C., Xie, C.M., Liu, Y.M., Xu, J.X., & Chen, J.W. (2017) Remnants of Late Permian–Middle Triassic Ocean islands in northern Tibet: implications for the late-stage evolution of the Paleo-Tethys Ocean. Gondwana Research, 44, 7-21.

Farooqui, M.A., Umar, M., Sabir, M.A., Pervez, R. & Jalees, T. (2019) Geochemical attributes of late Neoproterozoic Salt Range Formation, Pakistan: constraints on provenance, paleoclimate, depositional and tectonic settings. Geosciences Journal, 34(**2**): 201218.

Farooqui, M.A., Rehman, K.,Yaseen, A., Roohi, G., & Umar, M. (2022) Petrography, geochemistry and depositional model of Ispikan Conglomerate, Makran Accretionary Prism, Southwest Pakistan. Kuwait Journal of Science, 49 (**1**),1-25.

Flügel, E. (2004) Microfacies of carbonate rocks: analysis, interpretation and application. Springer, New York, 976.

Gaetani, M., & Garzanti, E. (1991) Multicyclic history of the northern India continental margin (northwestern Himalaya). Bulletin of American Association of Petroleum Geologists, 75(**9**), 1427-1446.

Gee, E.R. (1980) Pakistan Geological Salt Range Series: Directorate of Overseas Surveys, United Kingdom, for the Government of Pakistan, and Geological Survey of Pakistan, 6 sheets, scale 1:50,000.

Ghosh, N., Basu, A.R., Bhargava, O.N., Shukla, U.K., Ghatak, A., Garzione, C.N., & Ahluwalia, A.D. (2016) Catastrophic environmental transition at the Permian-Triassic Neo-Tethyan margin of Gondwanaland: Geochemical, isotopic and sedimentological evidence in the Spiti Valley, India. Gondwana Research, 34, 324-345.

Haq, B.U., Hardenbol, J., & Vail, P.R. (1988) Mesozoic and Cenozoic chronostratigraphy and cycles of sea-level change. In: Wilgus, C.K., Hastings, B.S., Kendall, C.G. St. C., Posamentier, H.W., Ross, C.A., Van Wagoner, J.C. (eds.) Sea-Level Changes: An Integrated Approach. Special Publication, No. 42. Society of Economic Paleontologists and Mineralogists, Tulsa. 71–108.

Haq, B.U., & Huber, B.T. (2017) Anatomy of a eustatic event during the Turonian (Late Cretaceous) hot greenhouse climate. Science China Earth Sciences, 60(**1**), 20-29.

Iqbal, S., Jan, I.U., & Hanif, M. (2014) The Mianwali and Tredian formations: An example of the Triassic progradational deltaic system in the low-latitude western Salt Range, Pakistan. Arabian Journal for Science and Engineering, 39(**7**), 5489-5507.

Kasi, A.K., Kassi, A.M., Umar, M., Friis, H., Mohibullah, M., & Mannan, A.R. (2018) A Paleogeographic and Depositional Model for the Neogene Fluvial Succession, Pishin Belt, Northwest Pakistan: Effect of Post Collisional Tectonics on Sedimentation in a Peripheral Foreland Setting. Acta Geol Sinica, 92(**2**), 499-518.

Khan, M.M.S.S., Jadoon, Q.A., Umar, M. & **Khan, A.A. (2021)** Microfacies, diagenesis and hydrocarbon Potential of Eocene carbonate strata Pakistan. Carbonates and evaporates, 36(**48**), 1-21.

Lawa, F.A., Koyi, H., & **Ibrahim, A.O. (2013)** Tectono-stratigraphic evolution of the NW segment of the Zagros fold belt, Kurdistan Region. Journal of Petrol Geology, Oxford Blackwell publishing, 36 (**1**), 75-69.

Marcoux, J., & Baud, A. (1996) Late Permian to Late Triassic Paleo-environments. Three snapshots: Late Murgabian, Late Anisian, Late Norian. The Tethys Ocean, Plenum Press, New York, 153-190.

Milsom, C., & **Rigby, S. (2010)** Fossils at a glance: John Wiley & Sons, 170.

Mukherjee, S. (2017) Shear heating by translational brittle reverse faulting along a single, sharp and straight fault plane. Journal Earth System Science, 126(**2**), 1-5.

Nazir, J., Ali, M., Sana, E., Ahmad, Q.A., Ghaffari, A., Basit, A., Javed, S., Ahmad, R., Ali, B., & **Rehman, N.U. (2020)** AVO analysis of Post-Stack Seismic data of Cretaceous Lumshiwal Formation in Kabirwala Block, Central Indus Basin Pakistan. Journal of Himalayan Earth Sciences, 53(**2**), 70-77.

Omar, A.A., Lawa, F.A., & **Sulaiman, S.H. (2015)** Tectonostratigraphic and structural imprints from balanced sections across the north-western Zagros fold-thrust belt, Kurdistan region, NE Iraq. Arabian Journal of Geosciences, 8(**10**), 8107-8129.

Qureshi, K., Shah, M.R., Meerani, I.A., Basit, A., Fahad, S., Shah, A.A., & **Hussain, H. (2019)** Hydrocarbon source and reservoir rock potential of Paleocene Hangu Formation in the Himalayan Foreland Basin, North West Pakistan: insight from geochemical and diagenetic study. Pakistan Journal of Scientific & Industrial Research, 62A (**3**), 157-166.

Sardar A.M., Soreghan, G.S., Heavens, N.G., Voeten, D.F.A.E., & **Ivanova, R.M. (2019**) Warm-water carbonates in proximity to Gondwanan ice–sheets: A record from the Upper Paleozoic of Iran. Palaeogeography Palaeoclimatology Palaeoecology, 531, 108914.

Scholle, P.A., & **Ulmer-Scholle, D.S. (2003)** A color guide to the petrography of carbonate rocks: grains, textures, porosity, diagenesis. American Association of Petroleum Geologists Memoir, 77.

Torsvik, T.H., & **Cocks, L.R.M. (2013)** Gondwana from top to base in space and time. Gondwana Research, 24(**3-4**), 999-1030.

Tucker, M.E., Wright, V.P., & **Dickson, J.A.D. (2006)** Carbonate sedimentology: John Wiley & Sons, 496.

Umar, M., Khan, A.S., Kelling, G., & **Kassi, A.M. (2011)** Depositional environments of Campanian–Maastrichtian successions in the Kirthar Fold Belt, southwest Pakistan: Tectonic influences on Late Cretaceous sedimentation across the Indian passive margin. Sedimentary Geology, 237(**1-2**), 30-45.

Umar, M., Khan, A.S., Kelling, G., Friis., H., & **Kassi, A.M. (2016)** Reservoir attributes of a hydrocarbon-prone sandstone complex: case of the Pab Formation (Late Cretaceous) of southwest Pakistan. Arabian Journal of Geosciences, 9(**1**), 74-89.

Umar, M., Khan, A.A., Qasim, M., Sabir, M., Jadoon, I.A.K., Farooq, M., & **Jamil, M. (2020)** Sedimentology of Galdanian Formation Hazara Basin Lesser Himalaya Pakistan: The signatures of Cambrian-Ordovician Pan-African Orogeny. Himalayan Geology, 41, 93-104.

Wignall, P.B., & **Hallam, A. (1993)** Griesbachian (Earliest Triassic) palaeoenvironmental changes in the Salt Range, Pakistan and southeast China and their bearing on the Permo-Triassic mass extinction. Palaeogeography Palaeoclimatology, Palaeoecology, 102(**3-4**), 215-237.

Zeigler, P.A. (2015) Post-Hercynian plate reorganization in the Tethys and Arctic-North Atlantic domains, Triassic Jurassic Rifting: Continental Breakup and the Origin of the Atlantic Ocean and Passive Margins (ed.) Manspeizer W, Elsevier, 711–756.

Submitted: 21/08/2021
Revised: 03/02/2022
Accepted: 07/02/2022
DOI: 10.48129/kjs.16575